ELSEVIER

Journal of Power Sources 107 (2002) 24–33

JOURNAL OF POWER SOURCES

www.elsevier.com/locate/jpowsour

Extension of Newman's method to electrochemical reaction–diffusion in a fuel cell catalyst layer

Tianping Duan, John W. Weidner*, Ralph E. White

Department of Chemical Engineering, Center for Electrochemical Engineering, University of South Carolina, Columbia, SC 29208, USA

Received 4 September 2001; accepted 9 October 2001

Abstract

A numerical technique is developed for solving coupled electrochemical reaction–diffusion equations. Through analyzing the nonlinearity of the problem, a trial and error iterating procedure is constructed. The coefficient matrix is arranged as a tridiagonal form with elements of block matrix and is decomposed to *LU* form. A compact forward and backward substitution algorithm based on the shift of inversing block matrix by Gauss–Jordan full pivoting is developed. A large number of node points is required to converge the calculation. Computation experiences show that the iteration converges very quickly. The effects of inner diffusion on the electrochemical reaction are analyzed by numerical solutions. © 2002 Published by Elsevier Science B.V.

Keywords: Electrochemical reaction–diffusion; Non-linear analysis; Numerical algorithm; Convergence; Thiele modulus

1. Introduction

Industrial chemical reactions are usually accompanied with mass and energy transfer, either homogeneously or heterogeneously. Mathematical modeling for these processes is based on material and energy balance. One can generate a set of differential equations known as the reaction–diffusion problem. Owing to the strong nonlinearity of the reaction rate, mainly from the effect of temperature, reaction–diffusion equations are paid more attention in analyzing and designing chemical and catalytic reactors and are the major role in analyzing the nonlinear dynamic behaviors in reactor engineering. The same phenomena exist in electrochemical processes, with the add complexity of a varying potential field, and considerable research has been reviewed for electrochemical reactions occurring in the porous electrode [1].

Newman discussed the numerical solution of boundary-value problems consisting coupled ordinary differential equations which one can often met in chemical engineering science, and developed a unique technique to solve coupled, linear differential equations [2–4]. In his procedure, a large, sparse matrix was collapsed to a tridiagonal matrix with elements of block matrixes, which make it easy to be inversed in solving the algebraic equations transformed from the original differential equations. Accordingly, the subroutine in his numerical method is called Newman's Band(*j*). White discussed Newman's method, and promoted this technique for wide application [5–7]. However, for solving reaction–diffusion equations—the nonlinear two-point boundary value problem, respective trial and error algorithms are needed. Shooting methods, such as Runge–Kutta integration scheme, is a marching technique that must be backwards processed from end point to beginning point to avoid inherent instability. This method is commonly used, but it depends on a proper choice of the initial value at the ending point. Linearizing the nonlinear kinetics term that convert the nonlinear differential equations into a linear one is called the linearization trial-and-error technique, but it does not guarantee that all steady state solutions can be determined. Compared with these two methods, transforming the nonlinear differential equations into nonlinear algebraic equations that are then solved by the Newton method did not receive the appropriate attention because the calculating time and storage is greater.

In this paper, we extend Newmans's matrix method to solve coupled electrochemical reaction–diffusion equations—a coupled high nonlinear two-point boundary value problem that is encountered in modeling of a fuel cell catalyst layer. Based on Taylor expansion, a trial and error iteraction algorithm is developed for solving the nonlinear algebraic equations transformed from the electrochemical reaction–diffusion equations. Owing to the adoption of

* Corresponding author. Tel.: +1-803-777-3207; fax: +1-803-777-8265.
E-mail address: weidner@engr.sc.edu (J.W. Weidner).

0378-7753/02/$ – see front matter © 2002 Published by Elsevier Science B.V.
PII: S0378-7753(01)00969-7

Nomenclature

a	specific interfacial area (cm^{-1})
c_0	dimensionless form of C_{H^+} ($c_0 = C_{H^+}/C^0_{H_2}$)
c_1	dimensionless form of C_{H_2} ($c_1 = C_{H_2}/C^0_{H_2}$)
c_2	dimensionless electric potential in the solid matrix phase ($c_2 = nf\phi_1$)
c_3	dimensionless electric potential in the pore ionic phase ($c_3 = nf\phi_2$)
C_{H^+}	effective concentration of proton per unit volume of solution (mol cm^{-3})
C_{H_2}	effective concentration of hydrogen per unit volume of solution (mol cm^{-3})
$C^0_{H_2}$	initial effective concentration of hydrogen (mol cm^{-3})
D_{H_2}	effective diffusion coefficient of hydrogen in pore phase ($cm^2\ s^{-1}$)
$E^{0'}$	formal potential (V)
f	constant ($f = F/RT$ (V^{-1}))
F	Faraday's constant (96485 C $eq.^{-1}$)
i	total current density leaving the matrix phase (A cm^{-2})
i_1	superficial electronic current density in the matrix (A cm^{-2})
i_2	superficial ionic current density in pore phase (A cm^{-2})
I_{cell}	current density of fuel cell, defined as positive (A cm^{-2})
k^0	heterogeneous rate constant for hydrogen oxidation (cm s^{-1})
k_1	dimensionless parameter ($k_1 = nflI_{cell}/\sigma$)
k_2	dimensionless parameter ($k_2 = nflI_{cell}/\kappa$)
l	thickness of anode catalyst layer (cm)
$n = 2$	number of electrons transferred in electrode reaction (=2)
N_{H_2}	superficial flux density of hydrogen (mol $cm^{-2}\ s^{-1}$)
R	universal gas constant (8.314 J $mol^{-1}\ K^{-1}$)
R_{H_2}	electrode reaction rate of hydrogen, defined as positive (mol $cm^{-3}\ s^{-1}$)
T	absolute temperature (K)
U	dimensionless formal potential ($U = nfE^{0'}$)
x	dimensionless form of distance through porous electrode ($x = X/l$)
X	distance through porous electrode (cm)

Greek symbols

α	transfer coefficient
ϕ_1	electric potential in the solid matrix phase (V)
ϕ_2	electric potential in the pore ionic phase (V)
Φ	Thiele modulus ($\Phi^2 = al^2k^0/D_{H_2}$)
Φ_1	dimensionless parameter ($\Phi_1^2 = an^2fFk^0l^2C^0_{H_2}/\sigma$)
Φ_2	dimensionless parameter ($\Phi_2^2 = an^2fFk^0l^2C^0_{H_2}/\kappa$)
κ	effective conductivity of the pore ionic (proton) phase ($\Omega^{-1}\ cm^{-1}$)
σ	effective conductivity of the solid matrix ($\Omega^{-1}\ cm^{-1}$)

Newman's unique method, in each iteration loop a compact forward substitution can be processed. In each forward or backward substitution, we use Gauss–Jordan full pivoting technique to guarantee the numerical stability. The whole computing is very fast, even though we set 2000 node points to make the substitution effectively. For a general case of an electrochemical reaction–diffusion process in a fuel cell catalyst layer, just two iteration loops can converge the solution. Using this method to study the effect of Thiele modulus on the electrochemical reaction–diffusion process, some intrinsic phenomena due to the nonlinear behavior of the system is found by numerical solution that is beneficial to analyze and scale-up a fuel cell system.

2. Model equation

We consider for the isothermal hydrogen oxidation reaction occurring in a porous catalyst layer of a fuel cell anode.

$$H_2 \rightleftharpoons 2H^+ + 2e^- \tag{1}$$

A schematic representation of it is shown in Fig. 1. The catalyst layer is viewed as a continuum of two phases, each phase either a pure ionic or electronic conductor. The ionic phase is considered a cationic selective polymer, such as Nafion. Therefore, the proton concentration throughout the catalyst layer is fixed. This uniform electrolyte concentration means the superficial current density in the pore ionic phase is due only to ion migration. This is represented mathematically as

$$i_2 = -\kappa \frac{d\phi_2}{dX} \tag{2}$$

The rate at which ionic current enters the pore solution, di_2/dX, is proportional to the reaction rate on a volumetric basis that is expressed by Butler–Volmer expression (defining anodic current as positive) [8]

$$\frac{di_2}{dX} = nFR_{H_2} = anFk^0[C_{H_2}e^{(1-\alpha)nf(\phi_1-\phi_2-E^{0'})} - C_{H^+}e^{-\alpha nf(\phi_1-\phi_2-E^{0'})}] \tag{3}$$

The movement of electrons in the solid matrix phase of the porous electrode is governed by Ohm's law

$$i_1 = -\sigma \frac{d\phi_1}{dX} \tag{4}$$

The consequence of electroneutrality is that the divergence of the total current density is zero.

$$\frac{di}{dX} = \frac{di_1}{dX} + \frac{di_2}{dX} = 0 \tag{5}$$

The flux of dissolved hydrogen in the porous anode is determined by diffusion

$$N_{H_2} = -D_{H_2}\frac{dC_{H_2}}{dX} \tag{6}$$

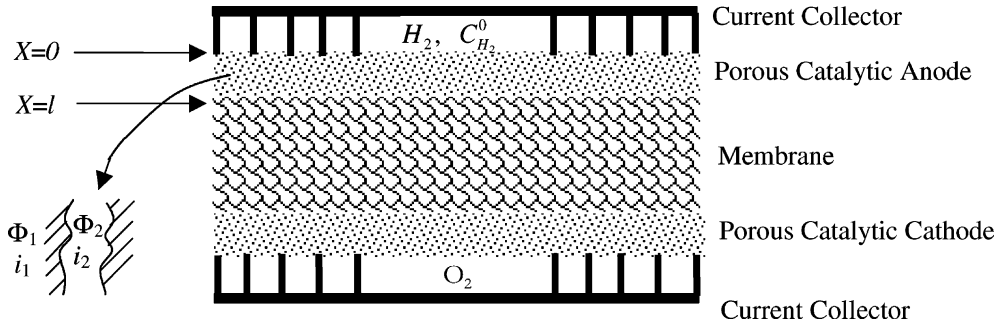

Fig. 1. Hydrogen oxidation in a fuel cell anode.

Material balance for this reaction–diffusion process can be modeled according to equation of continuity at steady state [9]

$$-\frac{dN_{H_2}}{dX} = R_{H_2} \tag{7}$$

Substituting Eq. (3), (6) into Eq. (7) yields

$$D_{H_2}\frac{d^2C_{H_2}}{dX^2} = ak^0[C_{H_2}e^{(1-\alpha)nf(\phi_1-\phi_2-E^{0'})} - C_{H^+}e^{-\alpha nf(\phi_1-\phi_2-E^{0'})}] \tag{8}$$

Differentiating Eqs. (2) and (4) and substituting Eq. (3) into the resulting equation gives

$$\sigma\frac{d^2\phi_1}{dX^2} = nFak^0[C_{H_2}e^{(1-\alpha)nf(\phi_1-\phi_2-E^{0'})} - C_{H^+}e^{-\alpha nf(\phi_1-\phi_2-E^{0'})}] \tag{9}$$

$$\kappa\frac{d^2\phi_2}{dX^2} = -nFak^0[C_{H_2}e^{(1-\alpha)nf(\phi_1-\phi_2-E^{0'})} - C_{H^+}e^{-\alpha nf(\phi_1-\phi_2-E^{0'})}] \tag{10}$$

Boundary conditions:

1. @ $X = 0$,

$$C_{H_2} = C^0_{H_2} \tag{11}$$

$$\frac{d\phi_1}{dX} = -\frac{I_{cell}}{\sigma} \tag{12}$$

$$\phi_2 = 0 \tag{13}$$

2. @ $X = l$,

$$\frac{dC_{H_2}}{dX} = 0 \tag{14}$$

$$\frac{d\phi_1}{dX} = 0 \tag{15}$$

$$\frac{d\phi_2}{dX} = -\frac{I_{cell}}{\kappa} \tag{16}$$

Setting the following dimensionless variables and parameters

$$c_0 = \frac{C_{H^+}}{C^0_{H_2}}, \quad c_1 = \frac{C_{H_2}}{C^0_{H_2}}, \quad c_2 = nf\phi_1, \quad c_3 = nf\phi_2,$$

$$x = \frac{X}{l}, \quad \Phi^2 = a\frac{k^0l^2}{D_{H_2}}\ (\text{Thiele modulus}), \quad U = nfE^{0'},$$

$$\Phi_1^2 = \frac{an^2fFk^0l^2C^0_{H_2}}{\sigma}, \quad \Phi_2^2 = \frac{an^2fFk^0l^2C^0_{H_2}}{\kappa},$$

$$k_1 = \frac{nfl}{\sigma}I_{cell}, \quad k_2 = \frac{nfl}{\kappa}I_{cell}$$

Then Eqs. (8), (10) and (11) are reduced to the dimensionless form

$$\frac{d^2c_1}{dx^2} = \Phi^2[c_1e^{(1-\alpha)(c_2-c_3-U)} - c_0e^{-\alpha(c_2-c_3-U)}] \tag{17}$$

$$\frac{d^2c_2}{dx^2} = \Phi_1^2[c_1e^{(1-\alpha)(c_2-c_3-U)} - c_0e^{-\alpha(c_2-c_3-U)}] \tag{18}$$

$$\frac{d^2c_3}{dx^2} = -\Phi_2^2[c_1e^{(1-\alpha)(c_2-c_3-U)} - c_0e^{-\alpha(c_2-c_3-U)}] \tag{19}$$

Boundary conditions:

1. @ $x = 0$,

$$c_1 = 1 \tag{20}$$

$$\frac{dc_2}{dx} = -k_1 \tag{21}$$

$$c_3 = 0 \tag{22}$$

2. @ $x = 1$,

$$\frac{dc_1}{dx} = 0 \tag{23}$$

$$\frac{dc_2}{dx} = 0 \tag{24}$$

$$\frac{dc_3}{dx} = -k_2 \tag{25}$$

Although the above model Eqs. (17)–(25) are for an isothermal system, due to the unique nonlinear characteristics of the electrochemical reaction term that is similar to the effect of temperature on a chemical reaction rate, the numerical solving method for these electrochemical reaction–diffusion equations can be transformed to study non-isothermal problems.

3. Numerical solution

For solving the model Eqs. (17)–(25), they are cast into sets of nonlinear algebraic equations approximated by finite difference. Then an iterative algorithm is constructed based on the Taylor expansion. However, if one adds the Eqs. (17)–(19) together to try to eliminate the nonlinear term, the computation is not stable. Analyzing the computing process on a microcomputer with eight word bits for a double precision real showed that the block matrixes were ill-conditioned. The condition numbers are too large to inverse the coefficient block matrixes correctly due to the error accumulation even for the second node point.

Therefore, at each node point except the boundary points, the second-order derivatives can be approximated by three point central difference accurate to $O(h^2)$. For example, Eq. (17) is approximated as

$$c_1(j-1) - 2c_1(j) + c_1(j+1) - h^2\Phi^2(c_1(j)e^{(1-\alpha)[c_2(j)-c_3(j)-U]} - c_0 e^{-\alpha[c_2(j)-c_3(j)-U]}) = 0 \tag{26}$$

If there are enough node points, we can suppose that the difference equation at node point j, such as Eq. (26), depends only on the variables at three points. If the left-hand term is expressed as $F_{1,j}$, then the Taylor series expands it to accuracy $O(h^2)$ as

$$\begin{aligned} &F_{1,j}(c_1(j-1), c_1(j), c(j+1), c_2(j), c_3(j)) \\ &\quad = c_1^0(j-1) - 2c_1^0(j) + c_1^0(j+1) \\ &\qquad - h^2\Phi^2[c_1^0(j)e^{(1-a)[c_2^0(j)-c_3^0(j)-U]} - c_0 e^{-\alpha[c_2^0(j)-c_3^0(j)-U]}] \\ &\qquad + [c_1(j-1) - c_1^0(j-1)]\frac{\partial F_{1,j}}{\partial c_{1,j-1}}\Big|_0 + [c_1(j) - c_1^0(j)]\frac{\partial F_{1,j}}{\partial c_{1,j}}\Big|_0 \\ &\qquad + [c_1(j+1) - c_1^0(j+1)]\frac{\partial F_{1,j}}{\partial c_{1,j+1}}\Big|_0 + [c_2(j) - c_2^0(j)]\frac{\partial F_{1,j}}{\partial c_{2,j}}\Big|_0 \\ &\qquad + [c_3(j) - c_3^0(j)]\frac{\partial F_{1,j}}{\partial c_{3,j}}\Big|_0 = 0 \end{aligned} \tag{27}$$

Substituting corresponding partial derivatives and introducing

$$\begin{aligned} r_0 &= e^{(1-\alpha)[c_2^0(j)-c_3^0(j)-U]}, \\ r_{j0} &= c_1^0(j)e^{(1-\alpha)[c_2^0(j)-c_3^0(j)-U]} - c_0 e^{-\alpha[c_2^0(j)-c_3^0(j)-U]}, \\ r_{c_0} &= (1-\alpha)c_1^0(j)e^{(1-\alpha)[c_2^0(j)-c_3^0(j)-U]} + \alpha c_0 e^{-\alpha[c_2^0(j)-c_3^0(j)-U]} \end{aligned} \tag{28}$$

it can be simplified as a more compact matrix form.

$$\begin{aligned} &[1 \quad 0 \quad 0]\begin{pmatrix} c_{1,j-1} \\ c_{2,j-1} \\ c_{3,j-1} \end{pmatrix} + [-(2+h^2\Phi^2 r_0) \quad -h^2\Phi^2 r_{c_0} \quad h^2\Phi^2 r_{c_0}]\begin{pmatrix} c_{1,j} \\ c_{2,j} \\ c_{3,j} \end{pmatrix} + [1 \quad 0 \quad 0]\begin{pmatrix} c_{1,j+1} \\ c_{2,j+1} \\ c_{3,j+1} \end{pmatrix} \\ &\quad = [-h^2\Phi^2 r_0 \quad -h^2\Phi^2 r_{c_0} \quad h^2\Phi^2 r_{c_0}]\begin{pmatrix} c_{1,j}^0 \\ c_{2,j}^0 \\ c_{3,j}^0 \end{pmatrix} + h^2\Phi^2 r_{j0}, \quad 0 < j < N \end{aligned} \tag{29}$$

In the same way, model Eqs. (18) and (19) can be approximated as Eqs. (30) and (31), respectively,

$$\begin{aligned} &[0 \quad 1 \quad 0]\begin{pmatrix} c_{1,j-1} \\ c_{2,j-1} \\ c_{3,j-1} \end{pmatrix} + [-h^2\Phi_1^2 r_0 \quad -(2+h^2\Phi_1^2 r_{c_0}) \quad h^2\Phi_1^2 r_{c_0}]\begin{pmatrix} c_{1,j} \\ c_{2,j} \\ c_{3,j} \end{pmatrix} + [0 \quad 1 \quad 0]\begin{pmatrix} c_{1,j+1} \\ c_{2,j+1} \\ c_{3,j+1} \end{pmatrix} \\ &\quad = [-h^2\Phi_1^2 r_0 \quad -h^2\Phi_1^2 r_{c_0} \quad h^2\Phi_1^2 r_{c_0}]\begin{pmatrix} c_{1,j}^0 \\ c_{2,j}^0 \\ c_{3,j}^0 \end{pmatrix} + h^2\Phi_1^2 r_{j0}, \quad 0 < j < N \end{aligned} \tag{30}$$

$$\begin{aligned} &[0 \quad 0 \quad 1]\begin{pmatrix} c_{1,j-1} \\ c_{2,j-1} \\ c_{3,j-1} \end{pmatrix} + [h^2\Phi_2^2 r_0 \quad h^2\Phi_2^2 r_{c_0} \quad -(2+h^2\Phi_2^2 r_{c_0})]\begin{pmatrix} c_{1,j} \\ c_{2,j} \\ c_{3,j} \end{pmatrix} + [0 \quad 0 \quad 1]\begin{pmatrix} c_{1,j+1} \\ c_{2,j+1} \\ c_{3,j+1} \end{pmatrix} \\ &\quad = [h^2\Phi_2^2 r_0 \quad h^2\Phi_2^2 r_{c_0} \quad -h^2\Phi_2^2 r_{c_0}]\begin{pmatrix} c_{1,j}^0 \\ c_{2,j}^0 \\ c_{3,j}^0 \end{pmatrix} - h^2\Phi_2^2 r_{j0}, \quad 0 < j < N, \end{aligned} \tag{31}$$

Letting

$$C(j) = (\, c_{1,j} \quad c_{2,j} \quad c_{3,j} \,)^{\mathrm{T}}, \quad 0 \le j \le N \tag{32}$$

then Eqs. (29)–(31) become

$$A(j)C(j-1) + B(j)C(j) + D(j)C(j+1) = G(j), \quad 0 < j < N, \tag{33}$$

in which

$$A(j) = \begin{pmatrix} 1 & 0 & 0 \\ 0 & 1 & 0 \\ 0 & 0 & 1 \end{pmatrix},$$

$$B(j) = \begin{pmatrix} -(2+h^2\Phi^2 r_0) & -h^2\Phi^2 r_{c_0} & h^2\Phi^2 r_{c_0} \\ -h^2\Phi_1^2 r_0 & -(2+h^2\Phi_1^2 r_{c_0}) & h^2\Phi_1^2 r_{c_0} \\ h^2\Phi_2^2 r_0 & h^2\Phi_2^2 r_{c_0} & -(2+h^2\Phi_2^2 r_{c_0}) \end{pmatrix},$$

$$D(j) = \begin{pmatrix} 1 & 0 & 0 \\ 0 & 1 & 0 \\ 0 & 0 & 1 \end{pmatrix},$$

$$G(j) = \begin{pmatrix} -h^2\Phi^2 r_0 & -h^2\Phi^2 r_{c_0} & h^2\Phi^2 r_{c_0} \\ -h^2\Phi_1^2 r_0 & -h^2\Phi_1^2 r_{c_0} & h^2\Phi_1^2 r_{c_0} \\ h^2\Phi_2^2 r_0 & h^2\Phi_2^2 r_{c_0} & -h^2\Phi_2^2 r_{c_0} \end{pmatrix} \begin{pmatrix} c_{1,j}^0 \\ c_{2,j}^0 \\ c_{3,j}^0 \end{pmatrix} + \begin{pmatrix} h^2\Phi^2 r_{j0} \\ h^2\Phi_1^2 r_{j0} \\ -h^2\Phi_2^2 r_{j0} \end{pmatrix} \tag{34}$$

Two-point boundary conditions are approximated by three point forward or backward difference accurate to $O(h^2)$ and are also expressed as a compact matrix form

$$B(0)C(0) + D(0)C(1) + XC(2) = G(0), \qquad j = 0 \tag{35}$$

and

$$YC(N-2) + A(N)C(N-1) + B(N)C(N) = G(N), \quad j = N \tag{36}$$

where

$$B(0) = \begin{pmatrix} 1 & 0 & 0 \\ 0 & 3 & 0 \\ 0 & 0 & 1 \end{pmatrix}, \qquad D(0) = \begin{pmatrix} 0 & 0 & 0 \\ 0 & -4 & 0 \\ 0 & 0 & 0 \end{pmatrix},$$

$$X = \begin{pmatrix} 0 & 0 & 0 \\ 0 & 1 & 0 \\ 0 & 0 & 0 \end{pmatrix}, \qquad G(0) = \begin{pmatrix} 1 \\ 2hk_1 \\ 0 \end{pmatrix} \tag{37}$$

$$Y = \begin{pmatrix} 1 & 0 & 0 \\ 0 & 1 & 0 \\ 0 & 0 & 1 \end{pmatrix}, \qquad A(N) = \begin{pmatrix} -4 & 0 & 0 \\ 0 & -4 & 0 \\ 0 & 0 & -4 \end{pmatrix},$$

$$B(N) = \begin{pmatrix} 3 & 0 & 0 \\ 0 & 3 & 0 \\ 0 & 0 & 3 \end{pmatrix}, \qquad G(N) = \begin{pmatrix} 0 \\ 0 \\ -2hk_2 \end{pmatrix} \tag{38}$$

Eqs. (33), (35) and (36) can be rewritten as a matrix form

$$\begin{bmatrix} B(0) & D(0) & X & & & & \\ A(1) & B(1) & D(1) & & & & \\ & \vdots & \vdots & \vdots & & & \\ & & A(j) & B(j) & D(j) & & \\ & & \vdots & \vdots & \vdots & & \\ & & & A(N-1) & B(N-1) & D(N-1) & \\ & & & Y & A(N) & B(N) & \end{bmatrix} \cdot \begin{bmatrix} C(0) \\ C(1) \\ \vdots \\ C(j) \\ \vdots \\ C(N-1) \\ C(N) \end{bmatrix} = \begin{bmatrix} G(0) \\ G(1) \\ \vdots \\ G(j) \\ \vdots \\ G(N-1) \\ G(N) \end{bmatrix} \tag{39}$$

The block matrixes $B(j)$ and vectors $G(j)$ at node points $0 < j < N$ are not determined due to the variables at expanded points (with superscript 0) being unknown. As a result, the tridiagonal matrix algebraic Eq. (39) cannot be solved directly. But if these unknown values at expanded points are guessed as trial values, then Eq. (39) can be solved. For a tridiagonal matrix algebraic equation, a compact forward and backward substitution algorithm can solve it quickly. This algorithm, at first, decomposes the tridiagonal matrix into a *LU* form. Then in the forward substituting, an intermediate vector will be acquired, and in the backward substituting, the variable vector can be obtained. In all the process of *LU* decomposition and forward and backward substitution, the Gauss–Jordan full pivoting algorithm is needed to inverse the block matrixes. Then the block matrix in the lower and upper matrix, the intermediate vector, and, at last, the variable vector can be solved. These solved variables are based on guessed values, they are not the real solution for the problem. They are set as new guessed values in the block matrixes $B(j)$ and $G(j)$ and reproduce the whole procedure. The iteration will not stop until the setting accuracy is reached, which makes the solutions satisfy the whole difference equations at each node point.

The procedure is illustrated as follows. When the values for determining the $B(j)$ and $G(j)$ are guessed, then the coefficient matrix in Eq. (39) can be decomposed

$$\begin{bmatrix} B(0) & D(0) & X & & & & \\ A(1) & B(1) & D(1) & & & & \\ & \vdots & \vdots & \vdots & & & \\ & & A(j) & B(j) & D(j) & & \\ & & \vdots & \vdots & \vdots & & \\ & & & A(N-1) & B(N-1) & D(N-1) & \\ & & & Y & A(N) & B(N) & \end{bmatrix}$$

$$= \underbrace{\begin{bmatrix} \bar{B}(0) & & & & & & \\ \bar{A}(1) & \bar{B}(1) & & & & & \\ & \vdots & \vdots & & & & \\ & & \bar{A}(j) & \bar{B}(j) & & & \\ & & & \vdots & \vdots & & \\ & & & & \bar{A}(N-1) & \bar{B}(N-1) & \\ & & & & \bar{Y}(N) & \bar{A}(N) & \bar{B}(N) \end{bmatrix}}_{L}$$

$$\cdot \underbrace{\begin{bmatrix} I & \bar{D}(0) & \bar{X} & & & & \\ & I & \bar{D}(1) & & & & \\ & & \vdots & \vdots & & & \\ & & & I & \bar{D}(j) & & \\ & & & & \vdots & \vdots & \\ & & & & & I & \bar{D}(N-1) \\ & & & & & & I \end{bmatrix}}_{U} \tag{40}$$

Through the shift of matrixes, the block matrix in the L and U matrixes can be solved. For $j = 0$, 1, we have

$$\bar{B}(0) = B(0), \qquad \bar{X} = \bar{B}^{-1}(0)X, \qquad \bar{D}(0) = \bar{B}^{-1}(0)D(0) \tag{41}$$

$$\bar{A}(1) = A(1), \qquad \bar{B}(1) = B(1) - A(1)\bar{D}(1),$$
$$\bar{D}(1) = \bar{B}^{-1}(1)D(1) - \bar{B}^{-1}(1)A(1)\bar{X} \tag{42}$$

As the same way, for other node points at$j = 2, \ldots, N-1$,

$$\bar{A}(j) = A(j), \qquad \bar{B}(j) = B(j) - \bar{A}(j)\bar{D}(j-1),$$
$$\bar{D}(j) = \bar{B}^{-1}(j)D(j) \tag{43}$$

can be solved. At the last node point $j = N$, we obtain

$$\bar{Y}(N) = Y, \qquad \bar{A}(N) = A(N) - \bar{Y}(N)\bar{D}(N-2),$$
$$\bar{B}(N) = B(N) - \bar{A}(N)\bar{D}(N-1) \tag{44}$$

Then Eq. (41) can be solved through the solution of two sets of matrix algebraic equations.

$$\underbrace{\begin{bmatrix} \bar{B}(0) & & & & & & \\ \bar{A}(1) & \bar{B}(1) & & & & & \\ & \vdots & \vdots & & & & \\ & & \bar{A}(j) & \bar{B}(j) & & & \\ & & & \vdots & \vdots & & \\ & & & & \bar{A}(N-1) & \bar{B}(N-1) & \\ & & & & \bar{Y}(N) & \bar{A}(N) & \bar{B}(N) \end{bmatrix}}_{L}$$

$$\cdot \underbrace{\begin{bmatrix} W(0) \\ W(1) \\ \vdots \\ W(j) \\ \vdots \\ W(N-1) \\ W(N) \end{bmatrix}}_{W} = \underbrace{\begin{bmatrix} G(0) \\ G(1) \\ \vdots \\ G(j) \\ \vdots \\ G(N-1) \\ G(N) \end{bmatrix}}_{G} \tag{45}$$

and

$$\underbrace{\begin{bmatrix} I & \bar{D}(0) & \bar{X} & & & & \\ & I & \bar{D}(1) & & & & \\ & & \vdots & \vdots & & & \\ & & & I & \bar{D}(j) & & \\ & & & & \vdots & \vdots & \\ & & & & & I & \bar{D}(N-1) \\ & & & & & & I \end{bmatrix}}_{U}$$

$$\times \underbrace{\begin{bmatrix} C(0) \\ C(1) \\ \vdots \\ C(j) \\ \vdots \\ C(N-1) \\ C(N) \end{bmatrix}}_{C} = \underbrace{\begin{bmatrix} W(0) \\ W(1) \\ \vdots \\ W(j) \\ \vdots \\ W(N-1) \\ W(N) \end{bmatrix}}_{W} \tag{46}$$

The intermediate vector $W(j)$, $j = 0, \ldots, N$ in Eq. (45) can be determined by forward substituting

$$W(0) = \bar{B}^{-1}(0)G(0) \tag{47}$$

$$W(1) = \bar{B}^{-1}(1)G(1) - \bar{B}^{-1}(1)\bar{A}(1)W(0) \tag{48}$$

$$W(j) = \bar{B}^{-1}(j)G(j) - \bar{B}^{-1}(j)\bar{A}(j)W(j-1) \tag{49}$$

$$W(N) = \bar{B}^{-1}(N)G(N) - \bar{B}^{-1}(N)\bar{Y}(N)W(N-2) - \bar{B}^{-1}(N)\bar{A}(N)W(N-1) \tag{50}$$

With backward substituting, the solution vector $C(j)$, $j = 0$, N are solved.

$$C(N) = W(N) \tag{51}$$

$$C(N-1) = W(N-1) - \bar{D}(N-1)C(N) \tag{52}$$

$$C(j) = W(j) - \bar{D}(j)C(j+1) \tag{53}$$

$$C(0) = W(0) - \bar{D}(0)C(1) - \bar{X}C(2) \tag{54}$$

The solved $C(j)$ are as new guessed values to determine the block matrixes $B(j)$ and $G(j)$, $j = 1, \ldots, N-1$ and to continually carry out the iteration, until the approximated solutions are obtained.

4. Results and discussion

4.1. Convergence

To test the solving technique, we chose a set of physical-chemical parameters shown in Table 1 that are common used for hydrogen oxidation in a fuel cell anode, then the following dimensionless model parameters are obtained

$$c_0 = 0.5714, \qquad \alpha = 0.5, \qquad U = 0,$$
$$\Phi^2 = 0.1406, \qquad \Phi_1^2 = \Phi_2^2 = 0.8277$$

Different currents density (0.2–1.6 A cm^{-2}) at two-point boundary that make k_1 and k_2 change between 0.2191–1.7526 were adopted. A Fortran 95 code was developed to do the numerical solution on a micro computer (Dell, Dimension 4100, Pentium III, 260 MB memory). After the number of node points was determined and a set of proper initial values were guessed for each variables at all the node points, the iterating process was carried out. It converged very quickly in just two loops. The numerical results are illustrated as Figs. 2–5.

It was found that a large number of node points, for example, >1000, is required to converge the iteration. We set it as 2000. Setting too many node points is the need for our assumption in the Taylor expansion that the nonlinear difference equation at node point j, depends only on variables at the three points. The iteration precision was chosen as 10^{-4}. The zero in the right-hand side of the sets of nonlinear algebraic equations in the form of Eq. (26) is approximated by this value. If all the absolute values of computation for the terms in the left-hand side are not $>10^{-4}$, then the iteration processes stop. For the case of 2000 node points, correspondingly, there are 6000 algebraic equations like Eq. (26) except those at the two-point boundary. Like all trial and error iteration algorithm, different initial estimations yield different results, in order to make the solution meet the physical meanings in the system, following current criteria are introduced in our computing to determine the initial trial solution and check the results

Table 1
Common physical–chemical parameters in modeling the hydrogen oxidation in a fuel cell anode

Parameter	Value
a (cm^{-1})	250
C_{H^+} (mol cm^{-3})	0.4×10^{-4}
$C^0_{H_2}$ (mol cm^{-3})	0.7×10^{-4}; 0.38×10^{-4} for $\Phi = 0.15$
D_{H_2} (cm^2 s^{-1})	2×10^{-4}
I_{cell} (A cm^{-2})	0.2–1.6
k^0 (cm s^{-1})	0.45
l (cm)	5×10^{-4}
T (K)	353.15
U	0
α	0.5
κ (Ω^{-1} cm^{-1})	0.3×10^{-1}
σ (Ω^{-1} cm^{-1})	0.3×10^{-1}

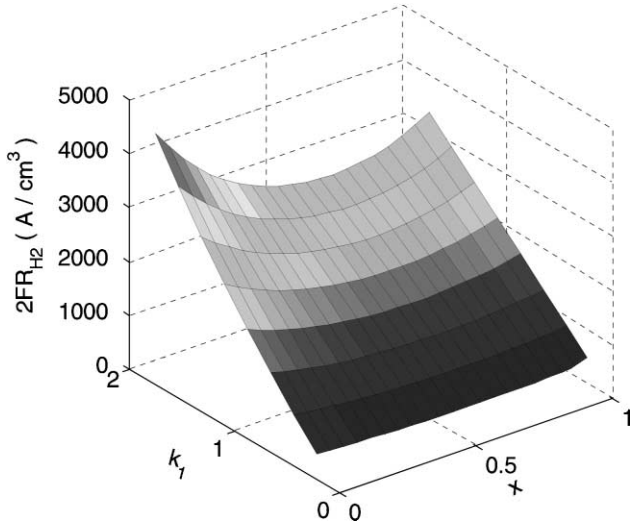

Fig. 2. Distribution of electrochemical reaction rate of hydrogen along x at different k_1 (current).

$$i_1 = -\sigma \left.\frac{d\Phi_1}{dX}\right|_{X=0} = I_{cell} \tag{55}$$

$$i_1 = -\sigma \left.\frac{d\Phi_1}{dX}\right|_{X=l} = 0 \tag{56}$$

$$i_2 = -\kappa \left.\frac{d\Phi_2}{dX}\right|_{X=l} = I_{cell} \tag{57}$$

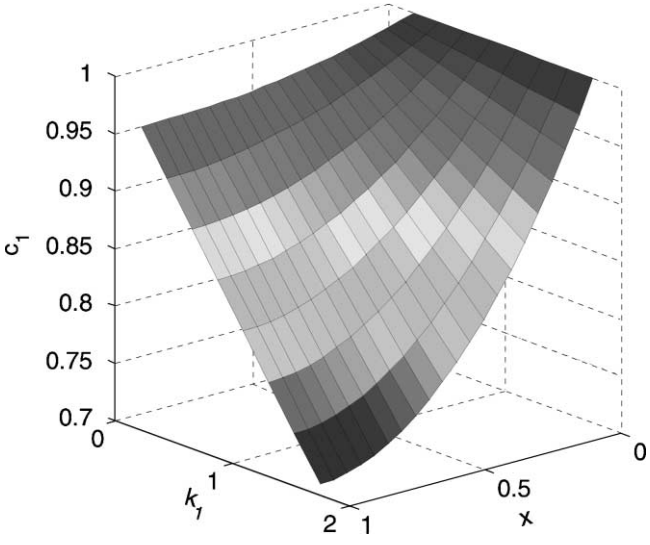

Fig. 3. Distribution of dimensionless hydrogen concentration c_1 along x at different k_1 (current).

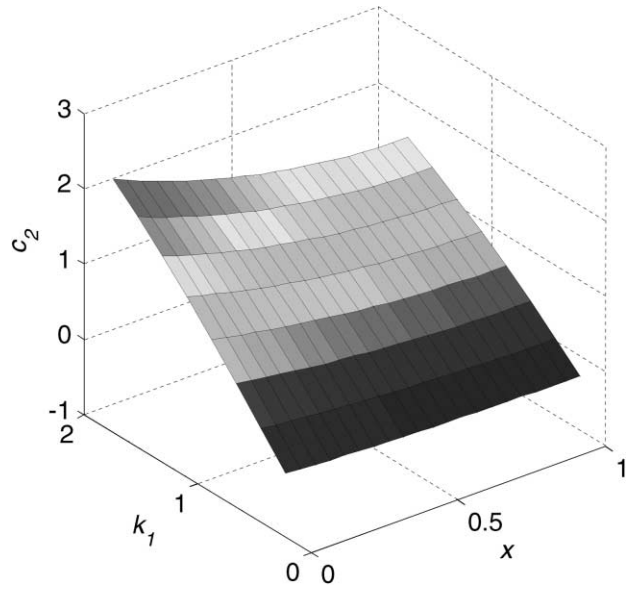

Fig. 4. Distribution of dimensionless potential in matrix along x at different k_1 (current).

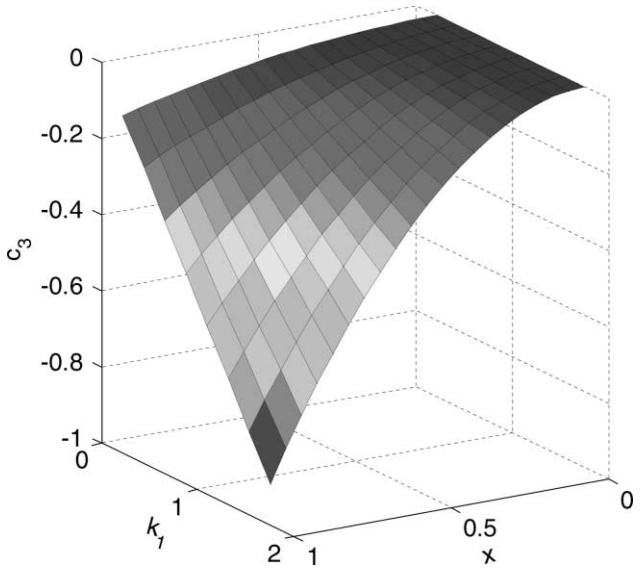

Fig. 5. Distribution of dimensionless potential in pore solution c_3 along x at different k_1 (current).

$$i_2 = -\kappa \left.\frac{\mathrm{d}\Phi_2}{\mathrm{d}X}\right|_{X=0} = 0 \tag{58}$$

$$I_{\mathrm{cell}} = \int_0^l \frac{\mathrm{d}i_2}{\mathrm{d}x}\,\mathrm{d}x \tag{59}$$

For Eqs. (55)–(58), the five point formula of numerical differential are adopted to calculate the potential gradient. For Eq. (59), complex Simposon's method is used to calculate the integration along the catalyst layer. All the calculations in these five equations are based on the data obtained from the numerical solution of the model equations.

4.2. Characteristics of electrochemical reaction–diffusion

The characteristics of reaction–diffusion problems are usually analyzed by the Thiele modulus Φ [10]. We changed the model parameters that is shown in Table 2 to get different Thiele modulus Φ in a range of 0.008–10, and corresponding electrochemical Thiele modulu Φ_1 and Φ_2 in a range of 0.01–8.06 and 0.02–10.95, respectively. The numerical solutions converge to the results very fast too, two loops of iteration for all case. The results are showed in Figs. 6–9.

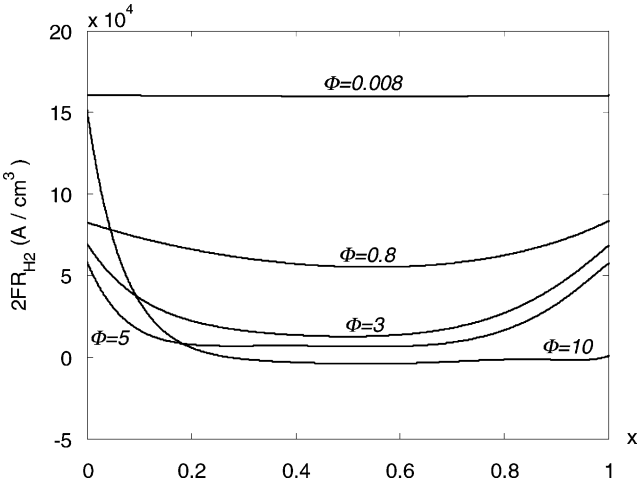

Fig. 6. Dependence of reaction rate on Thiele modulus, the parameters corresponding to these values of Φ are shown in Table 2.

When the Thiele modulus is low, such as $\Phi = 0.008$, the resistance of diffusion can be neglected, the distributions of reaction rate and hydrogen concentration are nearly uniform. When the Thiele modulus becomes larger, the diffusion

Table 2
Parameters for studying the dependence of hydrogen electro-oxidation reaction–diffusion on Thiele modulus in Figs. 6–9[a]

Φ	Φ_1	Φ_2	D_{H_2} (cm^2 s^{-1})	k^0 (cm s^{-1})	l (cm)	σ (Ω^{-1} cm^{-1})	κ (Ω^{-1} cm^{-1})
0.008	0.012	0.018	2.0×10^{-4}	0.45	0.1×10^{-4}	0.6×10^{-1}	0.3×10^{-1}
0.8	0.41	1.85	0.1×10^{-4}	0.4×10^{2}	0.25×10^{-4}	0.3×10^{-1}	0.15×10^{-2}
3	1.41	4.71	0.08×10^{-4}	0.8×10^{2}	0.6×10^{-4}	0.3×10^{-1}	0.268×10^{-2}
5	1.73	6.42	0.08×10^{-4}	0.8×10^{2}	1.0×10^{-4}	0.55×10^{-1}	0.40×10^{-2}
10	8.06	10.95	0.08×10^{-4}	0.8×10^{2}	2.0×10^{-4}	0.1×10^{-1}	0.55×10^{-2}

[a] Non-changing parameters: $C_{H^+} = 0.4 \times 10^{-4}$ mol cm^{-3}; $C_{H_2} = 0.65 \times 10^{-4}$ mol cm^{-3}; $I_{\mathrm{cell}} = 1.6$ A cm^{-2}; $T = 353.15$ K; $U = 0$; $a = 0.5$.

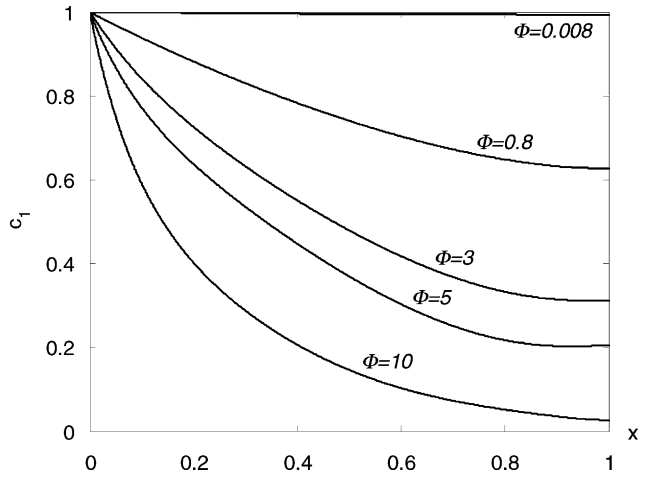

Fig. 7. Dependence of dimensionless hydrogen concentration on Thiele modulus, the parameters corresponding to these values of Φ are shown in Table 2.

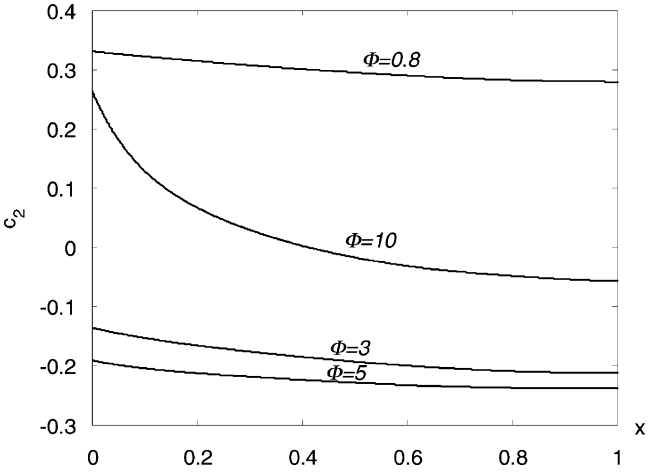

Fig. 8. Dependence of dimensionless potential in matrix on Thiele modulus, the parameters corresponding to these values of Φ are shown in Table 2.

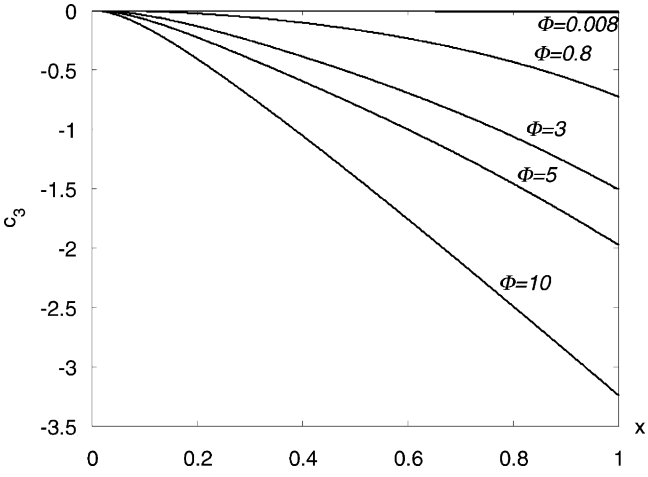

Fig. 9. Dependence of dimensionless potential in solution on Thiele modulus, the parameters to these values of Φ are shown in Table 2.

resistance increases, as a result, the reaction is not uniform along the catalyst layer, the larger the Thiele modulus is, the more non-uniform the reaction rate is. When the Thiele modulus is equal to 10, the reaction rate and hydrogen concentration decreases rapidly in the region near the surface of porous catalyst layer. It should be pointed out that in high Thiele modulus region, the rate of mass transfer by diffusion cannot meet the rate of electrochemical reaction, the process will lose its stability and become a dissipative system. As the same case in the stability issues in chemical reaction engineering, our numerical computing also found sensitive dependence of the solution results on some parameters when the Thiele modulus is high. It has been reported by a large amount of literature that in open chemical reaction system, especially coupled nonlinear chemical reaction and diffusion occur simultaneously, many complex phenomena will take place, such as multiple steady states, unstable states and self-generated sustained oscillations. Our present work just makes a beginning in this field, further attention should be paid to it because the electrochemical oxidation reaction rate of hydrogen is very fast under the catalysis of platinum catalyst. When a fuel cell stack is needed to scale up, it is necessary to know the dissipative behavior.

5. Conclusion

A numerical solution method is developed for coupled electrochemical reaction–diffusion equations. Even though the convergence of this technique depends mainly on the large number of node points, computation experiences on a microcomputer with double precision real only eight word bites shows that the procedure converges very fast. After the Taylor series is expanded and the corresponding iterating procedure is constructed, the computation process is stable. Arranging the elements in the coefficient matrix to block matrix form, the whole coefficient matrix is easily decomposed to lower and upper matrix, and the compact forward and backward substitution algorithm based on the shift of block matrixes with Gauss–Jordan full pivoting method can perform the numerical calculation quickly. Local convergence depends on the first trial solution, current criteria are required to make the solution converge to the correct results. It is suggested by the model solutions that dissipative behaviors in a electrochemical reaction–diffusion system might occur when the Thiele modulus is high.

Acknowledgements

This work was sponsored by the US Army Communications and Electronics Command under contact number (NRO-00-C-0134). The first author also got financial support from the China Scholarship Council (CSC, no. 99851035) and youth fund of Sichuan University.

References

[1] J. Newman, W. Tiedemann, AIChE J. 21 (1) (1975) 25.
[2] J. Newman, Ind. Eng. Chem. Fundam. 7 (1968) 514.
[3] J. Newman, Electrochem. Chem. 6 (1973) 187.
[4] J. Newman, Elctrochemical Systems, Appendix C, Prentice-Hall, Englewood Cliff, NJ, 1992, p. 539.
[5] R.E. White, Ind. Eng. Chem. Fundam. 17 (4) (1978) 367.
[6] D. Fan, R.E. White, Comput. Chem. Eng. 15 (11) (1991a) 797.
[7] D. Fan, R.E. White, J. Electrochem. Soc. 138 (6) (1991) 1688.
[8] A.J. Bard, L.R. Faulkner, Electrochemical Methods, Wiley, New York, 1980, p. 96.
[9] R.B. Bird, W.E. Stewart, E.N. Lightfoot, Transport Phenomena, Wiley, New York, 1960, p. 559.
[10] R. Aris, The Mathematical Theory of Diffusion and Reaction in Permeable Catalysts, Vol. I, Clarendon Press, Oxford, 1975, p. 40.